Radiotherapy and Oncology 174 (2022) 16–22

Contents lists available at ScienceDirect

Radiotherapy and Oncology

journal homepage: www.thegreenjournal.com

Original Article

MRI and FUNDUS image fusion for improved ocular biometry in Ocular Proton Therapy

Riccardo Via [a,*], Alessia Pica [a], Luca Antonioli [b], Chiara Paganelli [b], Giovanni Fattori [a], Chiara Spaccapaniccia [a], Antony Lomax [a], Damien Charles Weber [a,c,d], Ann Schalenbourg [e], Guido Baroni [d], Jan Hrbacek [a]

[a] Paul Scherrer Institut (PSI), Center for Proton Therapy, 5232 Villigen PSI, Switzerland; [b] Dipartimento di Elettronica Informazione e Bioingegneria, Politecnico di Milano, Milano 20133, Italy; [c] Department of Radiation Oncology, University Hospital Zurich, Rämistrasse 100, 8091 Zurich; [d] Department of Radiation Oncology, University Hospital Bern, Freiburgstrasse 18, 3010, Bern; and [e] Department of Ophthalmology, University of Lausanne, Jules-Gonin Eye Hospital, FAA, Lausanne, Switzerland

ARTICLE INFO

Article history:
Received 21 January 2022
Received in revised form 6 May 2022
Accepted 24 June 2022
Available online 03 July 2022

Keywords:
Ocular Proton Therapy
Magnetic resonance imaging
Panoramic Fundus Photography
Multi-modality Image Fusion
Target Volume Definition

ABSTRACT

Introduction: Ocular biometry in Ocular Proton Therapy (OPT) currently relies on a generic geometrical eye model built by referencing surgically implanted markers. An alternative approach based on image fusion of volumetric Magnetic Resonance Imaging (MRI) and panoramic fundus photography was investigated.

Materials and methods: Eighteen non-consecutive uveal melanoma (UM) patients, who consented for an MRI and had their tumour base visible on panoramic fundus photography, were included in this comparative analysis. Through generating digitally-reconstructed projections from MRI images using the Lambert azimuthal equal-area projection, 2D-3D image fusion between fundus photography and an eye model delineated on MRI scans was achieved and allowed for a novel definition of the target base (MRI + F_{CTV}). MRI + F_{CTV} was compared with MRI-only delineation (MRI_{CTV}) and the conventional (EyePlan) target definition (EP_{CTV}).

Results: The combined use of fundus photography and MRI to define tumour volumes reduced the average discrepancies by almost 65% with respect to the MRI only tumour definitions when comparing with the conventionally planned EP_{CTV}. With the proposed method, shallow sub-retinal tumour infiltration, otherwise invisible on MRI, can be included in the target volume definition. Moreover, a novel definition of the fovea location improves the accuracy and personalisation of the 3D eye model.

Conclusion: MRI and fundus image fusion overcomes some of the limitations of ophthalmological MRI for tumour volume definition in OPT. This novel eye tumour modelling method might improve treatment planning personalisation, allowing to better anticipate which patients could benefit from prophylactic treatment protocols for radiation induced maculopathy.

© 2022 The Authors. Published by Elsevier B.V. Radiotherapy and Oncology 174 (2022) 16–22

Ocular Proton Therapy (OPT) is a distinctive form of radiation therapy specifically tailored and designed for the treatment of intraocular lesions [1–3]. Several aspects make OPT unique even in the varied world of radiation therapy. The patient first undergoes a pre-treatment surgical procedure where tantalum markers (clips) are sutured to the outer sclera to mark the tumour base using transillumination. Patient anatomy and pathology is then typically *not* retrieved from volumetric imaging (CT or MRI), but is rather modelled geometrically and then adapted to a number of patient-specific parameters measured using ophthalmic imaging techniques (ultrasound, fundus photography). Treatment planning is predominantly performed using dedicated systems, the first of which, EYEPLAN, is still in widespread use today [4,5].

Though the clip surgery represents an additional burden for the patient and the reliability of the clip positioning depends on the surgeon's ability and experience, this procedure has led to universally excellent clinical results in terms of local tumour control rates [1,3], with a global average of local recurrence of only 4.2% [6] and, in consequence, avoiding an increase in metastatic risk linked to failure of the conservative eye treatment [7].

Despite its success, there are areas where Ocular Proton Therapy (OPT) can be improved. Recent research efforts to improve the treatment and treatment planning process have mainly been focused on the development of more sophisticated algorithms for dose calculation [8,9], the introduction of diagnostic volumetric imaging (CT & MRI) for eye modelling [10–14] or the combination of the two [15,16]. Also, there is a wide array of non-invasive ophthalmological imaging techniques such as colour fundus photography, ultrasound imaging, angiography and Optical Coherence

* Corresponding author at: WMSA/C29, 5232 Villigen PSI, Switzerland.
E-mail address: riccardo.via@psi.ch (R. Via).

https://doi.org/10.1016/j.radonc.2022.06.021
0167-8140/© 2022 The Authors. Published by Elsevier B.V.

Tomography, which provide a much higher resolution than CT and MRI, even if they only cover a limited portion of the eye [17,18].

Currently, panoramic fundus photography is the diagnostic imaging modality of choice. Unfortunately, the limited accuracy of the EyePlan geometrical eye model restricts its use to qualitative evaluations. While EYEPLAN allows for the registration of fundus images for validation purposes, it is seldomly used to define the clinical tumour volume [19], let alone to specify the location of structures at risk of radiation damage such as the optic disc or fovea [20,21]. Thus, the volumetric information provided by MRI specifically could complement the description of the tumour shape and volume [13,12,14] as well as improve the accuracy when localizing the macula and the optic nerve. However, delineation of the gross tumour volume using MRI imaging alone is not sufficiently accurate, due to its limited spatial accuracy, e.g. hindering the identification of shallow tumour infiltrations below the retinal surface [14].

In this study we present a multi-modality ophthalmological imaging approach for improved ocular biometry in Proton Therapy. Based on the proposed method, ocular features not directly discernible on 1.5T MRI scans, but appreciable on panoramic fundus photography such as the fovea and shallow sub-retinal tumour infiltration, can be integrated with an MRI-based eye model. This approach aims to overcome the limitation of ophthalmological MRI scans, while improving patient-specificity in definition of the fovea, with the goal of achieving a non-invasive, robust and accurate description of the eye anatomy and pathology for Ocular Proton Therapy.

Materials and methods

Patient dataset

Between 2017 and 2020, uveal melanoma scheduled for proton therapy at the PSI were proposed to undergo a 1.5T MRI orbital scan (3D volumetric T1-weighted Interpolated Breath-hold Examination-VIBE, 0.5 mm isotropic resolution, see [14]) following ethical approval (EKNZ 2014-217 and EKNZ 2019-01987). Thirty-seven, non-consecutive UM patients consented and as a consequence their fundus images, acquired with PANORET-1000 (Medibell Medical Vision Technologies, Haifa, Israel), were assessed. The Panoret camera is a trans-pupillary, hand-held digital imaging system using corneal contact lens and trans-scleral illumination. It features a 100° field-of-view and produces comprehensive colour images in the RGB spectrum reflected by the fundus [22].

Amongst the thirty-seven include patients, four (11%) presented lesions hardly visible either on fundus photography or MRI scans due to their anterior location (3 patients) of limited height (1 patient), respectively. For fifteen patients (41%) fovea and optic disk visibility on fundus photography was compromised by tumour infiltration. The remaining eighteen patients (49%) were included in this study as the tumour base (partial or entire), together with the optic disk and fovea, were visible on their panoramic fundus image. Three out of eighteen (17%) underwent an additional protocol, involving the administration of gadolinium as contrast agent to enhance tumour visibility.

Technique of MRI and Fundus image fusion

The geometrical fusion of fundus images with a three-dimensional model of the eye, derived from 1.5T MRI scans poses two main challenges. (1) A solution to the *ocular fundus projection* problem, i.e. the act of mapping the curved surface of a 3D spheroid, the retina and choroid, upon the 2D plane of the panoramic fundus photography, and (2) a *fusion* of this with the MR data. Our solution to these two problems is presented in the following sections.

The ocular fundus projection

Any geometrical transformation used to project a spherical surface onto a bi-dimensional plane introduces some sort of distortion [23]. Similarly, when a trans-pupillary fundus image is taken, the resulting picture will be affected by geometrical distortions associated with the process. Further complications arise from the coupling of the camera optics with the patient's eye, which can be considered as an additional optical system with its own individual optical properties. In addition, the air-to-cornea interface or the angle and inclination of the sensor at time of image acquisition are, amongst others, additional factors contributing to distortions in fundus images.

To address this issue, an empirical approach has been adopted based on using the Panoret-1000 fundus camera to acquire images of three custom-made spherical phantoms and compare three different projection methods (see Appendix, [29]).

Fusion of fundus images and MRI volumes

The distortions associated with the ocular fundus projection step, together with inherent unknowns of the fundus camera geometry, preclude the application of a rigorous Euclidean transformation for alignment with volumetric MR data. To overcome this, an image-based approach, exploiting intensity information in the MRI scans, has been developed and tested (Fig. 1).

For this, a fundus image (MRI-vF) is first digitally reconstructed from the MRI data by the projection of the scleral surface of the 3D MRI model upon a 2D plane which simulates the position of the fundus camera sensor. An intensity level is assigned to each point of the scleral surface by averaging the values of the five most proximal MRI voxels along a ray pointing at the scleral surface from the eye centre, retrieved by fitting a sphere to the eye globe (Fig. 1A). Then, using cubic interpolation and bi-dimensional Gaussian filtering, a virtual image is created, which can be directly compared to the original fundus image (PAN-F) to perform the fusion.

Ideally, a landmark-based approach for registration should be adopted for such a fusion, in which relevant features visible on both imaging modalities, for example the optic disk and the fovea, would be used to identify the best affine transformation (scale and orientation) for alignment. Due to the limits in resolution however (0.5 mm isotopic voxel size), such small ocular structures are not directly visible on the MRI scan. While the optic disk can be indirectly approximated as the intersection of the optic nerve and the sclera, there are no ancillary structures enabling a plausible definition of the fovea position on MRI. According to the literature, the position of the fovea varies from individual to individual and is defined by the angle (the so-called kappa angle) between the visual axis, where the macula lies, and the pupillary axis, i.e. the axis of eye symmetry [24,25]. Based upon these considerations, a fovea probability region can be defined on the MRI volumes as the intersection between the retinal surface and a cone with its vertex at the lens centre. This region encompasses the pupillary axis and assumes a deliberately overestimated range of variability ±9° (Fig. 1B). Any point belonging to this area is a fovea candidate and can be used in combination with the fixed position of the optic disk to register, on a patient-specific basis, the virtual (MRI-vF) and original (PAN-F) fundus images (Fig. 1C).

Thus, digitally reconstructed fundus images (MRI-vF) were qualitatively compared with actual fundus photographs (PAN-F) for all patients included in the study. A manual selection was performed aiming to have the best overlap of macroscopic part of the lesion on both images while thin lesion extensions were ignored as

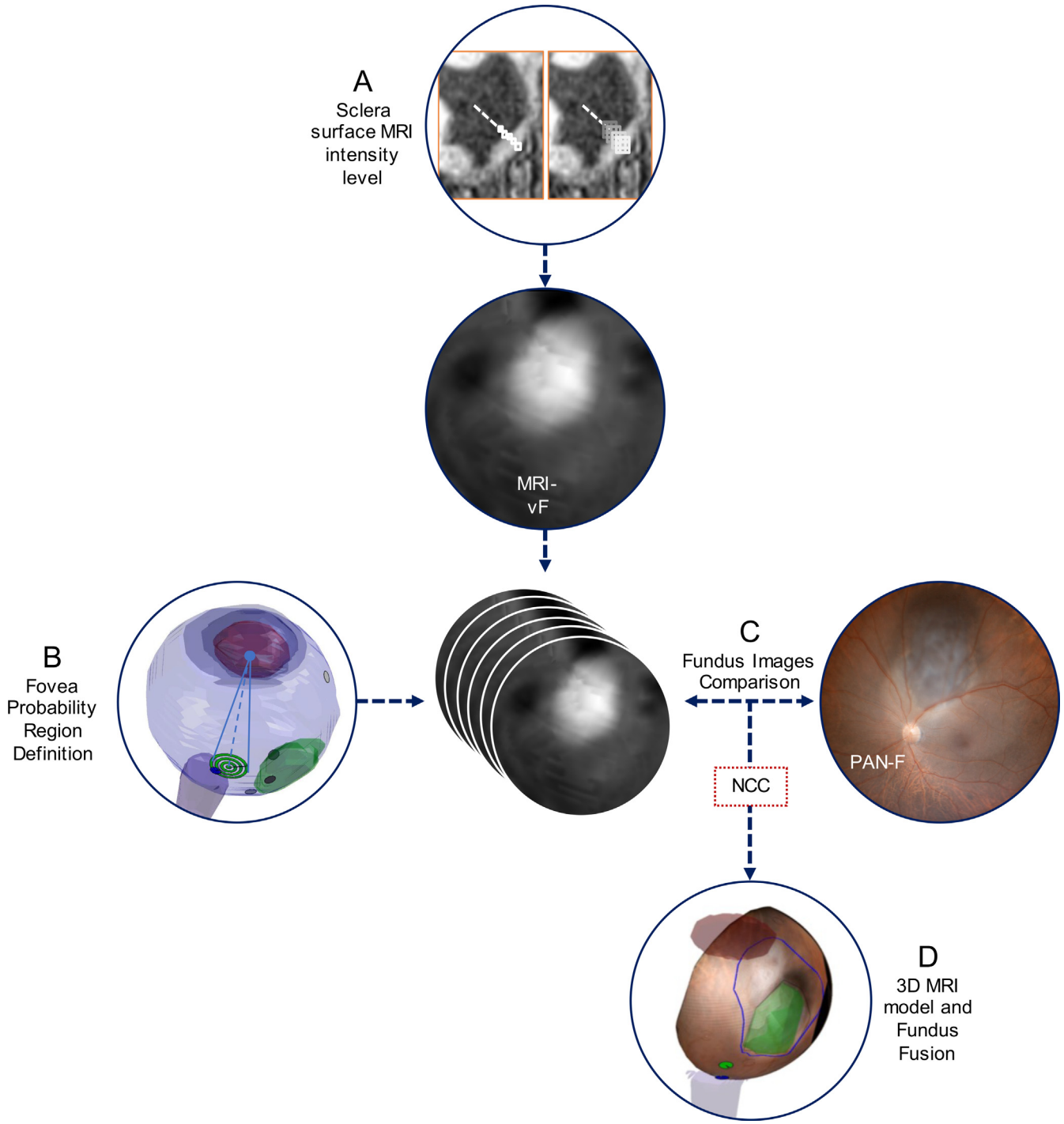

Fig. 1. A schematic representation of the method for fusion of the MRI-based 3D eye model and the Fundus photography.

not observable in MRI. Then, Normalized Cross Correlation (NCC) was calculated between the chosen MRI-vF and PAN-F images.

Comparative study on tumour volume definition and fovea position using combined MRI and fundus imaging data vs MRI only vs EyePlan

The identification of the virtual fundus photography most similar to the clinical picture leads to the consolidation of a reliable geometrical relationship between the fundus photography and the 3D MRI volume using Equation 1. Based on the fusion of the fundus image and MR, the tumour base delineation on the fundus image is propagated upon the 3D eye model and integrated with the tumour volume identified on the MRI scans to achieve a multi-modality, clinical tumour volume (MRI + F_{CTV}). Similarly, the patient's fovea, as identified on the fundus image, is back-projected on the 3D eye model (Fig. 1D). This was compared against conventional EYEPLAN treatment planning and the consensus guidelines for CT and MR atlas-based delineation in Neuro-Oncology recently proposed by the European Particle Therapy Network (EPTN) [26].

MRI + F_{CTV} was compared with MRI-only delineation (MRI_{GTV}) and conventional target volume definition (EP_{CTV}) based on clips using Volume Ratio (VR), Area Ratio (AR) and tumour-to-clip distances.

Results

The Lambert Azimuthal equal-area projection exhibited the lowest errors and as a result was adopted as the fundus projection technique throughout this study (see Appendix).

Eighteen out of the 37 UM patients (49%) satisfied the requirements of feature visibility in their fundus image and were therefore included in this analysis. Their EP_{CTV} volumes and tumour heights ranged from 84 to 2647 mm^3 and 2.5 to 7.1 mm, respectively. The identification of the MRI-vF best resembling the PAN-F was achieved for all patients with an average NCC coefficient of 0.47 (±0.07). However, the process was found to be particularly challenging for shallow tumours (tumour height < 3.0 mm). A significant correlation between high similarity of MRI-vF and PAN-F after registration, quantified using NCC, and tumour height was found (Pearson's rho coefficient: 0.80, *p*-value <0.005).

The results of the comparison of tumour volumes defined using the proposed method, compared to those defined in EYEPLAN (EP_{CTV}), are reported in Table 1.

When comparing the per-operative measurements of clip-to-tumour distances, the combined use of fundus photography and MRI to define tumour volumes reduced the average discrepancies by almost 65% with respect to the MR only tumour definitions (0.66 mm ± 1.80 mm and 1.80 mm ± 1.47 mm on average for MRI + FCTV and MRIGTV, respectively). Fig. 2 depicts the root mean square of clips discrepancies for MRI + F_{CTV} and MRI_{GTV} for all patients included in the dataset.

As seen in Fig. 2, P7 and P8 stands out as the two cases with the highest discrepancy. Here, the combination of fundus and MRI images clearly identified shallow sub-retinal infiltrations of the

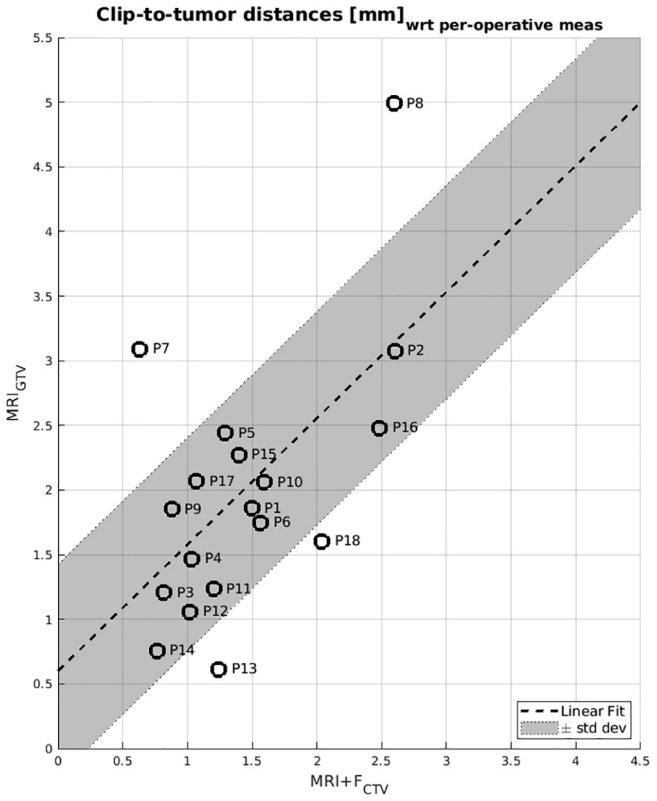

Fig. 2. Room Mean Square of clips-to tumour distances discrepancies between measurement performed at time of surgery and the tumour volume definition, based on MRI-only delineation (*y*-axis) and based on MRI and Fundus image fusion (*x*-axis) for the eighteen patients included in the study. Dotted line represent the linear fit of all data. The shaded grey area corresponds to the interval defined by the linear fit plus/minus the standard deviation of the discrepancies.

Table 1
Discrepancies in Tumor Volume Definition for ocular Proton Therapy. A gross target volume defined solely on MRI scans (MRI_{GTV}) and a clinical target volume defined using MRI in combination with Fundus photography using the proposed method (MRI + F_{CTV}) are compared with clips-based definition of the tumor extension using the treatment planning system EyePlan (EP_{CTV}). Also, the discrepancy in the fovea location determined using MRI in combination with Fundus and defined in the EyePlan model along with its distance to the Optic Disk are reported.

	Target Volume					Fovea Location	
Patient	Height [mm]	Volume Ratio		Area Ratio		MRI + F vs EP [mm]	MRI + F OD-Fovea distance [mm]
		MRI_{GTV}/EP_{CTV}	MRI + F_{CTV}/EP_{CTV}	MRI_{GTV}/EP_{CTV}	MRI + F_{CTV}/EP_{CTV}		
P1	3.88	0.47	0.50	0.55	0.57	0.43	4.93
P2	3.10	0.35	0.43	0.42	0.48	0.65	3.78
P3	2.15	0.50	0.56	0.57	0.76	1.17	3.39
P4	2.02	0.38	0.58	0.48	0.86	2.95	3.69
P5	4.18	0.39	0.52	0.51	0.80	1.13	4.24
P6	5.89	0.72	0.83	0.70	0.91	1.65	5.04
P7	2.75	0.33	0.65	0.36	0.93	0.67	3.85
P8	3.50	0.21	0.38	0.26	0.64	1.62	4.07
P9	3.01	0.37	0.52	0.38	0.59	1.75	3.89
P10	3.55	0.58	0.78	0.75	0.80	1.71	2.99
P11	3.37	0.69	0.72	0.77	0.83	2.33	5.36
P12	2.03	0.71	0.86	0.89	1.06	1.47	5.58
P13	5.4	1.00	1.09	1.04	1.25	2.32	4.86
P14	9.6	1.14	1.28	1.10	1.13	0.82	4.95
P15	4.0	0.73	1.04	0.64	0.94	3.28	5.66
P16	3.8	0.50	0.56	0.45	0.45	0.76	5.16
P17	7.1	0.83	1.00	0.91	1.14	1.72	3.75
P18	7.1	0.37	0.92	0.61	1.66	1.59	5.64
Mean	4.85	0.57	0.73	0.59	0.87	1.55	4.49
Std.Dev	1.83	0.25	0.26	0.25	0.30	0.79	0.85
			+16% ± 12%		+27% ± 26%		

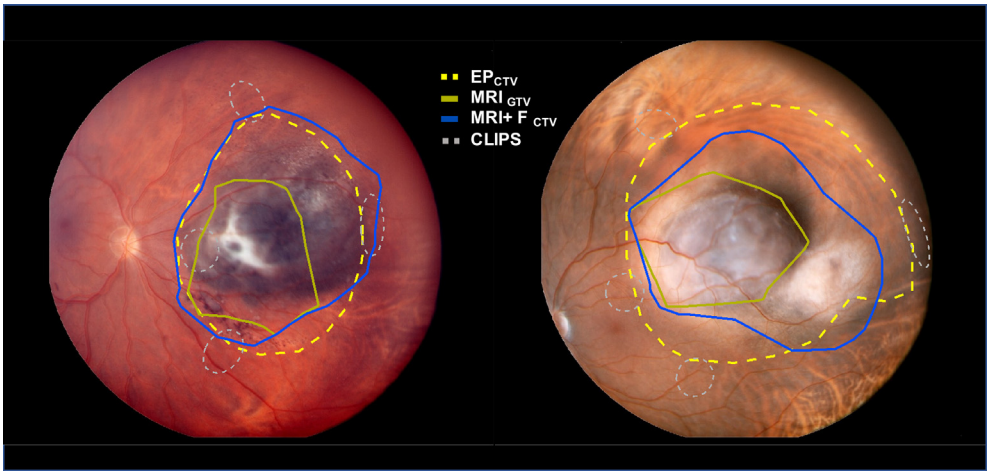

Fig. 3. Representation of the tumour base outline for Target Volume Definitions based on EyePlan (EP_{CTV}), MRI scans only (MRI_{GTV}) and the proposed method for integration of fundus photography information upon the MRI eye model (MRI + F_{CTV}) in two exemplary cases. The projection of the tantalum markers inserted in the pre-treatment clinical procedure is marked with a dotted grey line. Through delineation on 1.5T MRI scan, the target base, as seen on fundus photography is not entirely included in the target volume (solid dark-yellow line). The subretinal tumour infiltrations visible on fundus are too shallow to be visible with 3D ophthalmologic MRI imaging thus leading to potential tumour miss. On the contrary, through the combination with fundus photography (blue line), as well as using the conventional method based on clips (dashed yellow line), the entire base of the lesion is included in the tumour volume definition.

tumour which were otherwise invisible on the MRI images alone (see Fig. 3).

For 16 out of 18 (89%) of the cases, the fovea position, as determined from fundus image fusion, was inside the area defined by the EPTN guidelines. In comparison, for the conventional EyePlan definition, the fovea was outside of this same region in 44% (8/18) of the considered cases.

Fig. 4 shows two exemplary cases (P4 and P11, see Table 1) for which the difference in fovea location between the two eye models (EP and MRI + F) is above 2 mm and therefore fundus registration

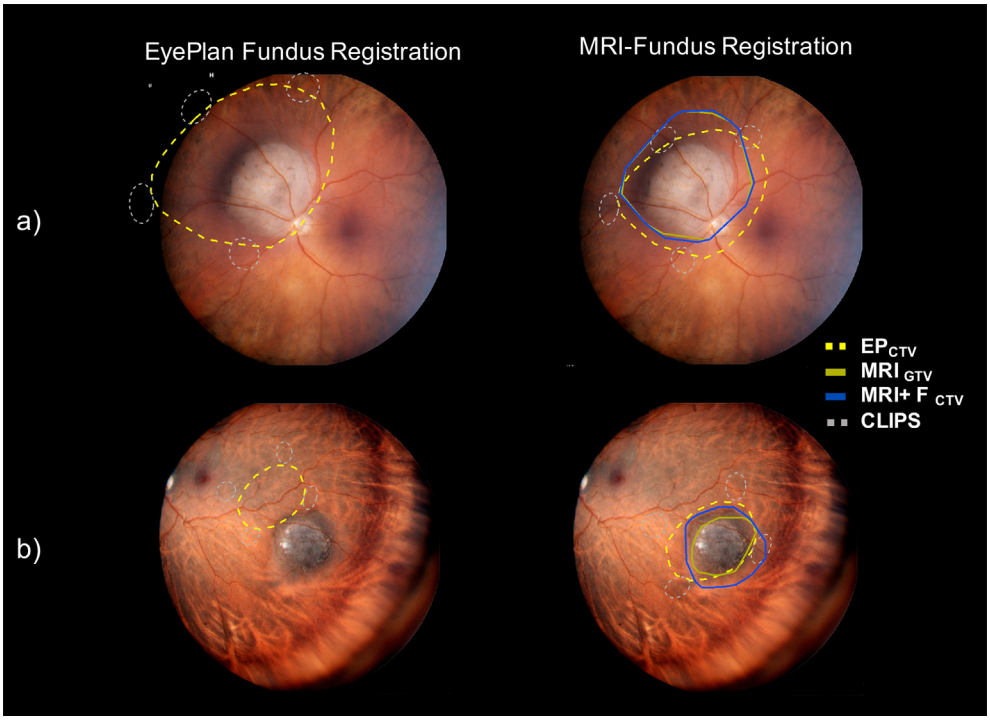

Fig. 4. Target Volume Definitions based on EyePlan (EP_{CTV} dotted yellow line), MRI scans only (MRI_{GTV} solid dark yellow line) and the proposed method (MRI + F_{CTV} solid blue line) for P4 and P11. The dotted grey line represents clips position. On the left the eye model is registered to the fundus using EyePlan demonstrating the inaccuracy of the method. On the right, our new method for eye model fusion with Fundus photography is used. The dotted yellow line still represents the EyePlan tumour base. Specifically, on panel (a), the inaccuracy of the fovea geographical definition in the EyePlan model leads to an incorrect registration with the fundus photography (left panel) which might suggest an overestimation of the target defined using clips. When using the novel definition of the macula position (right panel), the alignment errors are mitigated. On panel (b), another exemplary case is shown. Here, the EyePlan target appears to be completely missing the tumour visible on fundus photography. Again, by using the presented method target volume definition is consistent to fundus photography. The discrepancy in the macula geographical definition between EyePlan and the proposed methods was 2.33 mm and 2.95 mm for case (a) and (b), respectively.

using EyePlan leads to inaccurate projections, which might be mistaken for target volume definition misses or overestimations during clip surgery.

Discussion

The aim of this study was to develop and test an image-based approach to the integration and depiction of the retina and choroid, as captured by panoramic fundus photography, to an MRI-based anatomically accurate three-dimensional model of the eye.

An important first step towards this goal was to adopt the Lambert Azimuthal Equal-Areal projection to model the distortion introduced by the geometry of fundus imaging (see Appendix). While a complete description of the optical system of the fundus camera at the time of acquisition might be theoretically more accurate, it is rather unfeasible in practice due to the number of inherent uncertainties associated with the panoramic fundus photography. As such, the adoption of a purely empirical approach to the problem, through the analysis of experimental data acquired with the same machine used on patients, allowed us to determine the best projection model and quantify the associated errors. These have been found, on average, to be within a clinically acceptable 0.5 mm. Second, instead of relying on the conventional predefined anatomical definition of the macula and optic disk of EyePlan [16,19], an image-based approach, fully exploiting the intensity level information offered by MRI scans, has been developed. A direct comparison, both qualitative and quantitative, between fundus images acquired on the patient, and a corresponding picture digitally reconstructed from MRI, allows to define the relative geometry between the MRI eye model and the fundus photography, thus enabling us to integrate the tumour base and fovea position from fundus images with the MRI 3D eye model. As a result, a clinical tumour volume based exclusively on MRI and fundus image information can be generated.

With respect to the gross tumour volume delineated on MRI scans only, MRI + F_{CTV} is more similar to the EyePlan target definition. More importantly, sub-millimetric discrepancies with tumour-to-clip distances measured at time of implantation, the only quantitative available data involved in the conventional definition of the target base, showed, for MRI + F_{CTV}, an improvement of almost 65% with respect to MRI_{GTV}. As shown in Fig. 3, two patients in the considered dataset presented a sub-retinal tumour infiltration. Due to careful placement of the clips such that they encompassed the zone of flat choroidal infiltration, the full tumour volume could be included in the EyePlan model. These infiltrations were not visible on the available MRI scans. However, when applying the presented non-invasive multi-modality image-based method however, the definition of the tumour base, as delineated on the fundus images, could be fully integrated to the MRI, thus also achieving a complete coverage of the lesion.

Another advantage associated with this MRI 3D eye model is the more accurate anatomical localisation of the fovea position with respect to the generic geometrical eye model, as evidenced by the comparison with the EPTN guidelines and the cases in Fig. 4. In addition to doubts about the correctness of surgical clip positioning, the accuracy of the fovea location can have consequences for treatment planning, when choosing the eye position depends on the projected radiation exposure to sensitive structures such as the fovea, whose irradiation is a negative predictive factor for long-term vision [20,21]. Also, recent prophylactic treatment protocols, consisting of 2–4 monthly intravitreal anti-VEGFs (anti-vascular endothelial growth factors) injections have been proven successful in preventing irreversible loss of vision in those patients where the macula had been irradiated [27]. And identifying those patients who might benefit from such intensive follow-up and treatment, is currently based on EyePlan and therefore susceptible to inaccuracies.

However, it is important to point out how this alternative eye tumour modelling does not allow to abandon clip surgery, which is not only required for treatment planning but also treatment delivery. Clips guarantees the utmost accuracy in the patient position, verified using radiographic imaging [28], thus avoiding a geographical miss and local recurrence with a significantly increased risk for systemic metastases [7]. Unless this problem is resolved, clip surgery remains indicated to ensure continuing high local tumour control.

A limitation of this study is that the number of patients included in the analysis of the performance was dependent on the visibility of features on the fundus images. Obtaining a panoramic fundus image which contains the macula, optic disk and entire target is not possible for all patients due to the limitation of the field-of-view of the camera (Panoret-1000 features a 100° field-of-view). On the other hand, the creation of a composite fundus image using acquisitions capturing different parts of the retina is common practice in ophthalmology and, even though it would require investigation, we believe that there are no technical reasons that would prevent the application of the proposed methods on such composite images.

Also, the height of the tumour is a limiting factor: it is reasonable to expect, that it would be impossible to generate virtual fundus images of sufficient quality if the tumour height is below 2 mm with the resolution of the presented 1.5T MRI protocol. Even for tumours up to 3 mm of height the use of contrast agent and the absence of motion artefacts in MRI scans become crucial to a successful application of the proposed method. As such, further efforts towards improving MRI imaging quality and automatizing the fusion process are foreseen in the near future. Finally, the supervised selection of the virtual fundus image featuring the highest similarity to the original image is highly reliant on the expertise and judgement of the radiation oncologists and ophthalmologists involved. Clinical target volumes in the field of ophthalmological oncology, particularly when considering the limited size of the volumes involved and the proximity of structures relevant for vision retention, will likely always benefit from close supervision by trained professionals.

Conclusion

An alternative method to accurately model the tumour and the eye in Ocular Proton Therapy, based on the combination of MRI and fundus imaging, is presented in this study. Merging the information provided by 3D ophthalmological MRI scans and high-resolution fundus photography allows for the inclusion of the shallowest features of the tumour inside the target volume definition, up to now only possible with the implantation of surgical markers. Moreover, a localization of the fovea position can also be achieved, significantly improving the anatomical accuracy and personalisation of the eye model used for treatment planning. The latter could allow to avoid unnecessary irradiation of the fovea in certain cases, or, when unavoidable, to identify those patients who might benefit from prophylactic anti-VEGFs intravitreal injection treatment protocols, to prevent irreversible vision loss due to radiation induced maculopathy.

Declaration of Interest

The authors declare that they have no known competing financial interests or personal relationships that could have appeared to influence the work reported in this paper.

Acknowledgments

The research leading to these results have been founded by Krebsliga Schweiz (Swiss Cancer League) under grant agreement KFS-4447-02-2018 and by Personalised Health and Related Technologies under grant agreement PHRT-524

Appendix A. Supplementary data

Supplementary data to this article can be found online at https://doi.org/10.1016/j.radonc.2022.06.021.

References

[1] Egger E, Zografos L, Schalenbourg A, Beati D, Bhringer T, Chamot L, et al. Eye retention after protonbeam radiotherapy for uveal melanoma. Int J Radiat Oncol Biol Phys 2003;55:867–80.
[2] Hrbacek J, Mishra KK, Kacperek A, Dendale R, Nauraye C, Auger M, et al. Practice Pattern Analysis of Ocular Proton Therapy Centers: The International OPTIC survey. Int J Radiat Oncol Biol Phys 2016;95:336–43.
[3] Kacperek A. Ocular Proton Therapy Centers. In: Ion Beam Therapy. Berlin Heidelberg: Springer-Verlag; 2012. p. 149–77.
[4] Goitein M, Miller T. Planning proton therapy of the eye. Med Phys 1983;10:275–83.
[5] Sheen M. Review of EYEPLAN at Clatterbridge. 38 PTCOG meeting, Chester, UK, 2003.
[6] Chang MY, McCannel TA. Local treatment failure after globe-conserving therapy for choroidal melanoma. Br J Ophthalmol 2013;97:804–11.
[7] The Ophthalmic Oncology Task Force. Local recurrence significantly increases the risk of metastatic uveal melanoma. Ophthalmolgy 2016;123:86–91.
[8] Koch NC, Newhauser WD. Development and verification of an analytical algorithm to predict absorbed dose distributions in ocular proton therapy using Monte Carlo simulations. Phys Med Biol 2010;55:833–53.
[9] Rethfeldt C, Fuchs H, Gardey K. Dose distributions of a proton beam for eye tumor therapy: Hybrid pencil-beam and ray-tracing calculations. Med Phys 2006;33:782–91.
[10] Daftari IK, Aghaian E, O'Brien JM, Dillon W, Phillips TL. 3D MRI-based tumor delineation of ocular melanomas and its comparison with conventional techniques. Med Phys 2005;32:3355–62.
[11] Oberacker E, Paul K, Huelnhagen T, Oezerdem C, Winter L, Pohlmann A, et al. Magnetic resonance safety and compatibility of tanatalum markers used in proton beam therapy for intraocular tumors: A 7.0 Tesla study. Magn Reson Med 2017;78:1533–46.
[12] Tsiapa I, Tsilimbaris M, Papdaki E, Bouziotis P, Pallikaris I, Karantanas A, et al. High resolution MR eye protocol optimization: Comparison between 3D-CISS, 3D-PSIF and 3D-VIBE sequences. Physica Med 2015;31:774–80.
[13] Slopsema R, Mamalui M, Bolling J, Flampouri S, Yeung D, Li Z, et al. Can CT imaging improve targeting accuracy in clip-based proton therapy of ocular melanoma? Phys Med Biol 2019;64:035010.
[14] Via R, Hennings F, Pica A, Fattori G, Beer J, Peroni M, et al. Potential and pitfalls of 1.5T MRI imaging for target volume definition in ocular proton therapy. Radiother Oncol 2020;154:53–9.
[15] Fleury E, Trnkovà P, Erdal E, Hassan M, Stoel B, Jaarma-Coes M, et al. Three-dimensional MRI-based treatment planning approach for non-invasive ocular proton therapy. Med Phys 2021;48:1315–26.
[16] Dobler B, Bendl R. Precise Modellig of the Eye for Proton Therapy of Intra-Ocular Tumours. Phys Med Biol 2002;47:493–613.
[17] Shields C, Furuta M, Thangappan A, Nagori S, Mashayekhi A, Lally D, et al. Metastasis of Uveal Melanoma Millimeter-by-Millimeter in 8033 consecutive Eyes. Arch Ophthalmol 2009;127:989–98.
[18] Shields C, Say E, Samara W, Khoo C, Masahyekhi A, Shields J. Optical coherence tomography angiography of the macula after plaque radiotherapy of choroidal melanoma. J Retinal Viterous Dis 2016;36:1493–505.
[19] Daftari IK, Mishra KK, O'Brien JM, Tsai T, Park SS, Martin S, et al. Fundus image fusion in EYEPLAN software: An evaluation of a novel technique for ocular melanoma radiation treatment planning. Med Phys 2010;37:5199–207.
[20] Thariat J, Grange J-D, Mosci C, Rosier L, Maschi C, Lanza F, et al. Visual Outcomes of Parapapillary Uveal Melanomas Following Proton Beam Therapy. Int J Radiat Oncol Biol Phys 2016;95:328–35.
[21] Pica A, Weber DC, Vallat L, Bergin C, Hrbacek J, Schweizer C, et al. Good long-term visual outcomes of parapapillary choroidal melanoma patients treated with proton therapy: a comparative study. Int Ophthalmol 2021;41:441–52.
[22] Schalenbourg A, Zografos L. Pitfalls in colour photography of choroidal tumours. Eye 2013;27:224–9.
[23] Snyder JP. Map Projections – A working Manual. Washington DC: U.S. Geological Survey Professional Paper; 1987.
[24] Artal P. Optics of the eye and its impact in vision: a tutorial. Adv Opt Photonics 2014;6:340–67.
[25] Schaeffel F. Kappa and Hirschberg ratio measured with an automated video gaze tracker. Optom Vis Sci 2002;79:329–34.
[26] Eekers DBP, Di Perri D, Roelofs E, Postma A, Dijkstra J, Ajithkumar T, et al. Update of the EPTN atlas for CT- and MR-based contouring in Neuro-Oncology. Radiother Oncol 2021;160:259–65.
[27] Eandi C, Polito M, Schalenbourg A, Zografos L. Eighteen-month results of intravitreal anti-vascular endothelial growth factor on vision and microcirculation in radiation maculopathy. Retina 2021;41:1883–91.
[28] Via R, Hennings F, Fattori G, Fassi A, Pica A, Lomax A, et al. Noninvasive eye localization in ocular proton therapy through optical eye tracking: A proof of concept. Med Phys 2018;45:2186–94.
[29] IOGP Publication 373-7-2. Coordinate Conversions and Transformation including Formulas. Geomatics Guidance Note Number 7, part 2; 2019.
[30] Rosca D, Plonka G. Uniform spherical grids via equal area projection from the cube to the sphere. J Comput Appl Math 2011;236:1033–42.